

# Mapping the receptor site for ergtoxin, a specific blocker of ERG channels

Liliana Pardo-López<sup>a</sup>, Jesús García-Valdés<sup>a</sup>, Georgina B. Gurrola<sup>a</sup>, Gail A. Robertson<sup>b</sup>,  
Lourival D. Possani<sup>a,\*</sup>

<sup>a</sup>Department of Molecular Recognition and Structural Biology, Institute of Biotechnology, National Autonomous University of Mexico, Avenida Universidad 2001, P.O. Box 510-3, Cuernavaca 62210, Mexico

<sup>b</sup>Department of Physiology, Wisconsin University, Madison Medical School, Madison, WI 53706, USA

Received 7 November 2001; accepted 19 November 2001

First published online 30 November 2001

Edited by Maurice Montal

**Abstract** We show here that ergtoxin (ErgTx) is a bona fide, specific blocker of the human ether-a-go-go-related gene (HERG) channels. It does not affect the function of either M-eag or M-elk channels. A chimeric construction containing a segment of the P-region of M-eag channel inserted into the HERG channel drastically diminished or completely abolished the inhibitory effect of ErgTx, whereas chimeras of the P-region of HERG channel into M-eag channels recovered the inhibitory effect. From the P-region point mutants of HERG channel assays, only the mutant N598Q shows about 25% decrement of the ErgTx inhibitory effect. ErgTx recognizes the P-region of HERG channels, blocking the channel function with a  $K_d$  in the order of 12 nM. © 2002 Published by Elsevier Science B.V. on behalf of the Federation of European Biochemical Societies.

**Key words:** Human ether-a-go-go-related gene channel; K<sup>+</sup> channel; Ergtoxin; M-elk channel; M-eag channel; Scorpion toxin

## 1. Introduction

The human ether-a-go-go-related gene (HERG) is a member of the Eag super family of genes encoding potassium channels with six transmembrane domains, an S4 region and a highly conserved P-region [1]. Mutations in HERG give rise to inherited, type 2 long QT syndrome [2], caused by a loss of the cardiac repolarizing current I<sup>Kr</sup> [3,4]. Currents arising from expression of HERG or ERG, as the homologs in other species are known, also play a role in spike-frequency adaptation in neurons [5] and in human pancreatic  $\beta$ -cells [6].

ERG channels are the target of a group of potent drugs including anti-arrhythmics, anti-histamines and antibiotics [7,8] that block K<sup>+</sup> currents causing acquired long QT syndrome as a side effect. The discovery of naturally occurring substances that can specifically and reversibly block or recognize these types of channels is fundamental for the search and development of new putative drugs to treat some of the diseases and malfunctions associated with HERG channels. For the voltage-dependent K<sup>+</sup> channels the use of scorpion toxins [9–11] has been extremely useful to determine the geometry of the outer vestibule of the pore of the channel, to conduct studies of double mutants (channel and toxin coding genes)

for correlation of the structure with the function of the ligand–receptor complexes [12–18]. Two main kinds of naturally occurring peptides from scorpions and spiders have been isolated and characterized: (i) the blocker toxin type, that interacts with the outer vestibule of the pore inhibiting the channels by physically occluding the K<sup>+</sup> conduction [19], in a 1:1 stoichiometric relationship, and (ii) the gating modifier, that interacts with the S3–S4 segments of the channel in a 1:4 stoichiometry relationship and modifies the closing and opening kinetics of the channel [20,21].

We have recently found ergtoxin (ErgTx) [22,23], the first scorpion peptide capable of blocking specifically ERG channels. In this communication we describe the interaction of ErgTx with three chimeras of HERG and M-eag channels and six different point mutants involving the P-region of the HERG channel.

## 2. Materials and methods

### 2.1. Preparation of chimeras and point mutants

The nomenclature for chimeras adopted in this communication was selected by using the first letter of each channel (either *H*, standing for HERG; or *M*, standing for M-eag; note the italics, which distinguish the letters from amino acid residues). Thus, *HMH* means a chimera where the upstream sequence of the gene encoding HERG channel was used, followed by a segment of the M-eag gene (here only sequences that encode the pore region of the channel) and the extending sequence to the end of the C-terminal region of the channel was again from HERG channels. Conversely, *MHM* means a construction of a chimeric gene where the N-terminal is from M-eag, the pore segment contains HERG gene sequence and the C-terminal is again from M-eag.

The cDNA for chimera *HMH* was constructed from two PCR reactions. The first amplified the pore of M-eag; a 5' end tag of HERG clone was introduced and a *Bgl*II site of M-eag 3' end was eliminated. The second PCR amplified the first product, using HERG channel as template; a *Bst*EII site of HERG clone was introduced. The PCR product (M-eag pore with 5' end of HERG) and the HERG clone into pCDNA3 were digested with *Bst*EII and *Bgl*II (a *Bgl*II site of pCDNA3 was eliminated). The final PCR product was then subcloned into the corresponding site of the HERG gene.

The encoded channel was composed of HERG sequences from the amino-terminus to residue C566, at which point it crossed over to M-eag residue I396. At M-eag residue K577, the sequence again crossed back to HERG at residue K638.

Chimeras *MHM* and *M382H* were constructed using an in vitro recombination technique as previously described by Herzberg et al. [24]. The first crossover point in the *MHM* construct occurs between M-eag residue V449 and HERG residue V611. The second crossover point occurs after HERG residue L650 to M-eag residue L498. For *M382H*, the crossover occurs between M-eag residue 382 and HERG residue M619.

\*Corresponding author. Fax: (52)-73-172388.

E-mail address: possani@ibt.unam.mx (L.D. Possani).

The point mutations of HERG gene were prepared by direct mutagenesis by two step PCR reactions in which appropriate primers were used. The correct presence of mutants was verified by sequencing the products in an automatic Applied Biosystems machine.

## 2.2. Toxin purification

ErgTx was purified by chromatographic procedures as earlier described [23].

## 2.3. Channel expression in oocytes

Complementary RNAs for injection into oocytes were synthesized from the T7 promoter of linearized DNA templates at the *PvuII* site using the Mmessage Mmachine kit (Ambion, Austin, TX, USA). The oocytes were prepared following the technique described earlier [24]. In brief, female *Xenopus laevis* frogs (Nasco) were anesthetized by 15 min exposure to 0.15% of 3-aminobenzoic acid ethyl ester (Sigma). The oocytes were surgically removed from the ovary, after which the frog was closed by suturing and placed in water to allow recovery from the anesthesia. Defolliculation was performed by incubation for 1 h in 1.5 mg/ml collagenase (Sigma Type II) in  $\text{Ca}^{2+}$ -free OR2 oocyte medium with gentle agitation. Oocytes were stored in ND96 solution (in mM): 96 NaCl, 2 KCl, 1  $\text{MgCl}_2$ , 1.8  $\text{CaCl}_2$ , 5 HEPES buffer adjusted to pH 7.4 with NaOH and supplemented with 10  $\mu\text{g/ml}$  gentamicin) at 18°C. Oocytes were injected with 50 nl of cRNA (0.3 ng/ml) by using a microdispenser and a micropipette. Injected oocytes were incubated at 18°C for 24–48 h in ND96 medium, before analysis.

## 2.4. Electrophysiological recordings

Channels were expressed to a level where 0.5–5.0  $\mu\text{A}$  of current was recorded during a depolarizing step from a holding potential of  $-80$  mV to potentials between  $-80$  and  $+60$  mV, and repolarizing at  $-100$  mV. Currents were recorded using the two-electrode voltage clamp method (CA-1B high performance oocyte clamp DAGAN). Electrodes were filled with 3 M KCl, had a resistance of 0.3–1.0 M $\Omega$ . The bath solution contained (mM) 95 NaCl, 5 KCl, 1  $\text{MgCl}_2$ , 0.3  $\text{CaCl}_2$ , 5 HEPES buffer adjusted to pH 7.4 with NaOH. Control records were taken prior to the addition of toxin. On the addition of toxin the perfusion medium was stopped to allow homogeneous dispersion of the toxin. In most experiments toxin was removed from the bath to demonstrate recovery.

## 3. Results and discussion

### 3.1. Specificity of ErgTx effect in oocyte expressed channels

ErgTx effects were originally reported on ERG-like currents in native neural and cardiac tissues and tissue-derived cell lines shown to express the gene encoding ERG [22]. In the present study we assessed the specificity of the ErgTx interaction by comparing its relative effects on heterologously expressed  $\alpha$ -subunits of HERG, M-eag and M-elk channels in *Xenopus* oocytes. The aim of this study was to determine whether ErgTx was specific for ERG and to identify the region of toxin binding on the channel. Fig. 1 shows the recordings of toxin effect (left panel control, right panel after toxin application) on M-eag channels (Fig. 1A), M-elk channels (Fig. 1B) and HERG channels (Fig. 1C). The current was decreased only for the HERG channels. Fig. 1D shows the current versus voltage profile of the inhibitory effect of ErgTx in HERG channels. Inhibition was almost fully reversible as shown in the figure by the circles. A dose–response curve for the effect of ErgTx (Fig. 1E) shows a  $K_d$  value of 11.4 nM. This ErgTx sensitivity is similar to that observed for ERG-like currents in native cells and cell lines (16 nM; see [22]). The M-eag and M-elk channels (Fig. 1A,B, respectively) were not inhibited, even after application of a toxin concentration in the range of 200 nM. These experiments were repeated several times ( $n=6$ ) with identical results. Our findings provide additional confirmation that the previously recorded native currents [22] arise from channels composed primarily of the ERG  $\alpha$ -subunit. The high sensitivity of HERG for the ErgTx also suggested that the heterologous expression system, together with manipulation of the HERG channel structure using recombinant DNA techniques, would provide a useful means by which to identify the binding domain of ErgTx on the HERG channel.

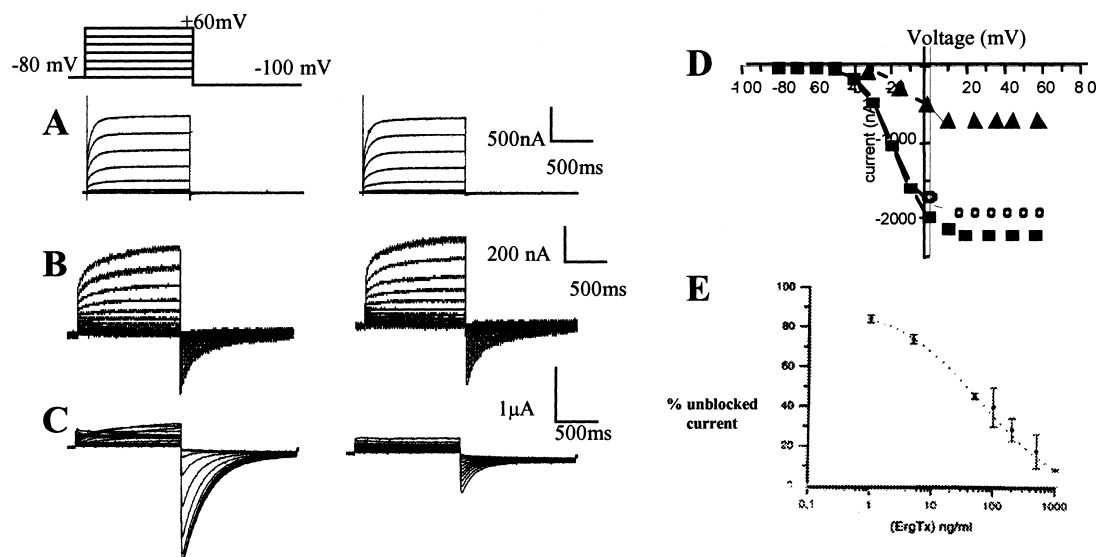


Fig. 1. Effect of ErgTx on three different  $\text{K}^+$  channels.  $\text{K}^+$  currents were measured in oocytes expressing: (A) M-eag, (B) M-elk and (C) HERG channels. Left panels are control recordings, right panels are in the presence of 100 nM ErgTx, from a holding potential of  $-80$  mV to  $+60$  mV by increments of 10 mV each, whereas the tail currents were elicited by repolarization to  $-100$  mV. Panel D represents a current versus voltage trace of the inhibitory effect of ErgTx on HERG channels, in which the squares are control traces, triangles are in the presence of toxin and circles are the recovery of currents after washing the toxin. Panel E is a dose–response curve for ErgTx on HERG channels. The calculated  $\text{IC}_{50}$  was 50 ng/ml ( $n=3$ ), using  $(1 + ([\text{ErgTx}]/\text{IC}_{50})^p)^{-1}$ ,  $P < 0.05$ .

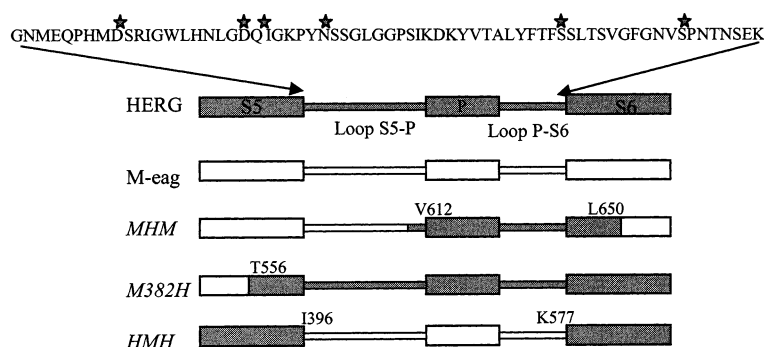


Fig. 2. Scheme showing the chimeric constructions and point mutants of HERG channels. Upper line shows the amino acid sequence of HERG channel from residue G572 to K638. The stars on top of amino acids indicate point mutations: D580A, D591A, I593R, N593Q, S620T and S631V. The subsequent lines show: (i) a schematic representation of HERG channel sequence from the S5 to S6 transmembrane regions (shadowed boxes), where the arrows show the position of the amino acids from G572 to K638; (ii) the equivalent scheme for the M-eag channel (empty boxes); (iii) the chimeric M-eag–HERG–M-eag channel, where the sequence from V612 to L650 is from HERG; (iv) the *M382H* chimeric construction in which the N-terminal is from M-eag up to T556 and the remaining sequence is from HERG and (v) the last chimeric is HERG sequence up to C566 and after K638, whereas the internal segment is from M-eag I396–K577.

### 3.2. Mapping the receptor site for ErgTx binding

We took advantage of the homology between HERG and M-eag to make chimeras and determine what regions of HERG uniquely specify ErgTx sensitivity (Fig. 2). Because previous studies have shown that other scorpion toxins bind to the pore region of voltage-gated  $K^+$  channels of the Kv family, we tested the hypothesis that the pore-forming region serves as the ErgTx binding site in HERG. According to this hypothesis, chimeric M-eag channels with an HERG pore should be inhibited by ErgTx. If the binding were in a different region of HERG, such as the S3–S4 loop serving as the spider hanatoxin receptor in  $K^+$  channels [20,21], sensitivity would be determined by the parent channel in regions outside the pore. Fig. 2 shows the chimeras schematically, with M-eag sequences in unfilled boxes and HERG sequences in filled boxes. We also tested six constructs with point mutations in the corresponding region, as indicated with asterisks.

As a model, we will refer to sub-domains of the bacterial channel KcsA pore, which have been structurally determined

[25]. Within the selectivity filter and preceding pore helix, there is a high degree of sequence similarity between KcsA, HERG and M-eag. In the upstream turret area, the sequence diverges among all three channels.

As a first test of the sensitivity of the pore region to toxin binding, we replaced the pore in HERG with the corresponding sequences of M-eag (*HMH*; Fig. 3). The *HMH* chimera is not sensitive to ErgTx. The currents were not modified in the presence of toxin. However, as it can be observed in Fig. 3C, the substitution of the pore region (M-eag into Herg) abolishes the rectification property of the channel. Fig. 3C does not show the effect of the toxin, but rather compares the behavior of the native M-eag (circles) with that of the chimera (triangles). This observation suggests that the amino acid sequence of the S5–P loop segment of HERG channel, although similar to that of M-eag in size, contains information or spatial folding that makes it different. ErgTx senses the difference between them.

To confirm that pore sequences of HERG were important

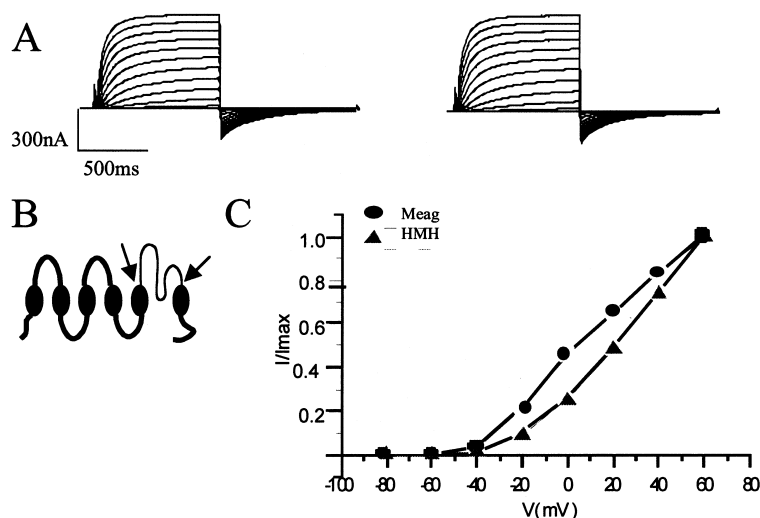


Fig. 3. Effect of ErgTx on *HMH* chimera. A: Left shows outward currents, under voltage clamp conditions for control recordings (similar to M-eag channel alone), and right is in the presence of 200 nM ErgTx. B: The scheme of the chimera (N-terminal and C-terminal of HERG in bold, middle section is from M-eag channels). C: Current versus voltage relationship of the outward currents of A compared with M-eag channels (circles), for  $n = 5$ .

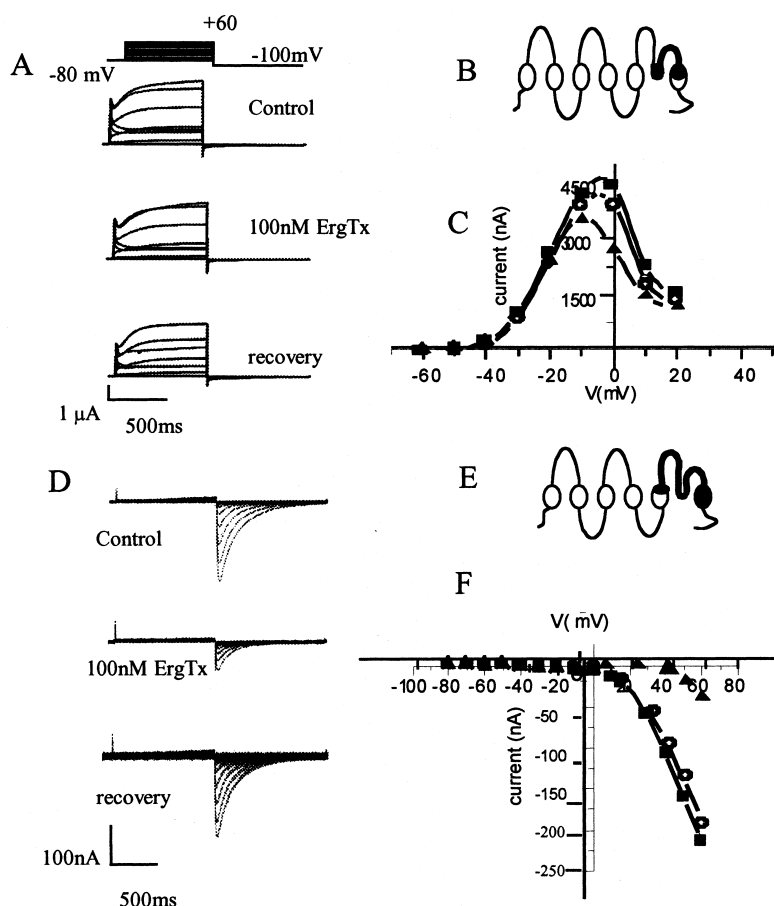


Fig. 4. Effect of ErgTx on *MHM* and *M382H* chimeras. A–C are from *MHM*, whose caricature is depicted in B (N-terminal of HERG and C-terminal from M-eag in bold), whereas D–F are from the *M382H* chimera, scheme shown in E. Panel A shows the outward currents elicited according to the protocol of Fig. 1, for control (upper recordings), after application of 100 nM ErgTx (middle) and after washing (lower panel). Panel C shows the current versus voltage curve of the results in A, where the squares represent the control, triangles the toxin effect and the open circles the washing condition ( $n=3$ ,  $P<0.005$ ). D: The same situation as A, for the *M382H*, and F is the corresponding current versus voltage curve, where the squares represent the recording of the control, triangles the toxin effect and the open circles the recovery ( $n=4$ ,  $P<0.02$ ).

in toxin binding, we studied the chimera *MHM*, an M-eag channel in which the P-region beginning between the turret and the pore helix, and extending half-way through S6, has been replaced with corresponding HERG sequences (see Section 2 and [24]). Despite possessing much of the HERG pore, *MHM* exhibited a drastically reduced sensitivity to ErgTx (Fig. 4A–C). Currents were reduced by only 15%, even at high toxin concentrations (100 nM). This chimera exhibits the rapid activation characteristic of M-eag and the rapid inactivation characteristic of HERG, resulting in a partially inactivating, large outward current intermediate between the two parental phenotypes (see also [24]). The intact inactivation indicates that the external mouth of the pore retains its normal function and suggests that the relative lack of toxin binding is not due to a general disruption of structure in that region.

Because *MHM* does not contain the entire HERG pore sequence, including the ‘turret’, we tested the sensitivity of the chimera *M382H*, which contains a pore composed entirely of HERG sequence. As shown in Fig. 4, *M382H* is clearly inhibited by ErgTx (Fig. 4D–F). This chimera exhibits the pronounced inward rectification characteristic of the wild-type HERG channel. The block is about 80%, using 100

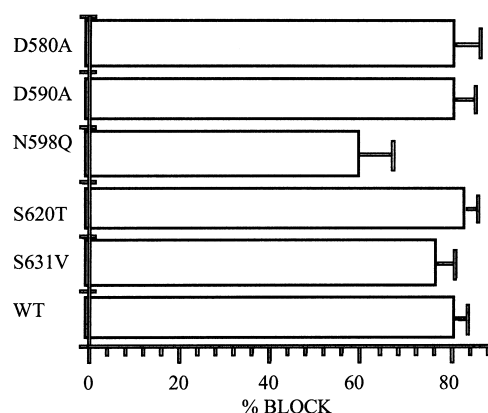


Fig. 5. Percent of blockage for the site-directed mutants. This graphic shows the percent of blockage due to the application of 100 nM ErgTx for the point mutants, shown on the left: D580A, D591A, N598Q, S620T, S631V and wild-type (WT). Error bars indicate mean ( $\pm$  S.E.M.,  $n=3$ ).

nM ErgTx, and it is reversible by washing. These observations strongly support a role for the HERG pore region in ErgTx block, especially in the highly divergent turret region that distinguishes HERG from M-eag, M-elk and other K<sup>+</sup> channels. Moreover, they exclude a primary role for residues in the HERG S3–S4 region in toxin binding.

Finally, we tested six point mutations in this region in an attempt to identify particular amino acids that specify the binding preference of ErgTx for HERG channel (see Fig. 5). Among the mutants tested, only N598Q showed a small reduction in inhibition by the toxin, exhibiting 60% compared with 80% inhibition of wild-type channels. However, this 25% reduction of inhibition should be taken only as an indication for the need of additional point mutation studies in this segment of the channel. I593R did not express. Surprisingly, mutations that disrupt C-type inactivation (and presumably the conformation of the outer pore region), S620T and S631V, had little effect on toxin inhibition of the current. Considering that agitoxin and charybdotoxin binding are disrupted by *Shaker* mutations equivalent to S631V, our findings suggest that their mechanisms of binding are likely to differ from that of ErgTx in HERG. Perhaps this should not be surprising, as the amino acid sequence of ErgTx is quite different from the other known Kv specific toxins (42 amino acids with four disulfide bridges; see [23]). More surprising may be the insensitivity of ERG channels to other K<sup>+</sup> channel toxins from scorpions, despite homology in the binding regions. One can speculate that structural differences, most notably the long sequence predicted to give rise to an unusually large turret (see review by Tseng [26]), present steric hindrance to an otherwise conserved binding site.

In conclusion, our results support the idea that ErgTx is specific for HERG channel and does not recognize other, closely related channels. It is a legitimate blocker of HERG, able to recognize the amino acid sequence between the S5–P loop region. The specific binding sites are either different from the location where other scorpion toxins bind to the Kv channels, or the structure of the S5–P loop region of HERG channel is different from that of the voltage-dependent K<sup>+</sup> channels. More mutagenesis studies will be required to pinpoint the residues specifying ErgTx block.

**Acknowledgements:** This work was partially supported by Grants from: Howard Hughes Medical Institute 55000574, DGAPA-National Autonomous University of Mexico, IN216900 and 31691-N from

CONACyT-Mexican Government to L.D.P. and NIH Grant HL55973 (G.A.R.). L.P.L. received a scholarship from CONACyT and DGAPA for her Ph.D. studies.

## References

- [1] Warmke, J.W. and Ganetzky, B. (1994) *Proc. Natl. Acad. Sci. USA* 91, 3438–3442.
- [2] Curran, M.E., Splawski, I., Timothy, K.W., Vincent, G.M., Green, E.D. and Keating, M.T. (1995) *Cell* 80, 795–803.
- [3] Sanguinetti, M.C., Jiang, C., Curran, M.E. and Keating, M.T. (1995) *Cell* 81, 299–307.
- [4] Trudeau, M.C., Wanke, J.W., Ganetzky, B. and Robertson, G.A. (1995) *Science* 269, 92–95.
- [5] Chiesa, N., Rosati, B., Arcangeli, A., Olivotto, M. and Wanke, E. (1997) *J. Physiol.* 501, 313–318.
- [6] Rosati, B., Marchetti, P., Crociani, O., Lecchi, M., Lupi, R., Arcangeli, A., Olivotto, M. and Wanke, E. (2000) *FASEB J.* 14, 2601–2610.
- [7] Roden, D.M. (1998) *Am. J. Cardiol.* 82, 491–571.
- [8] Mitcheson, J.S., Chen, J., Lin, M., Culbertson, C. and Sanguinetti, M.C. (2000) *Proc. Natl. Acad. Sci. USA* 97, 12329–12333.
- [9] Carbone, E., Wanke, E., Prestipino, G., Possani, L.D. and Maelicke, A. (1982) *Nature* 296, 90–91.
- [10] MacKinnon, R. and Miller, C. (1988) *J. Gen. Physiol.* 91, 335–349.
- [11] Miller, C. (1995) *Neuron* 15, 5–10.
- [12] MacKinnon, R. and Miller, C. (1989) *Science* 245, 1382–1385.
- [13] Goldstein, S.A. and Miller, C. (1993) *Biophys. J.* 65, 1613–1619.
- [14] Stocker, M. and Miller, C. (1994) *Proc. Natl. Acad. Sci. USA* 91, 9509–9513.
- [15] Hidalgo, P. and MacKinnon, R. (1995) *Science* 266, 307–310.
- [16] Krezel, A.M., Kasibhatla, C., Hidalgo, P., MacKinnon, R. and Wagner, G. (1995) *Protein Sci.* 4, 1478–1489.
- [17] Naranjo, D. and Miller, C. (1996) *Neuron* 16, 123–130.
- [18] Gross, A. (1996) *Neuron* 16, 399–406.
- [19] Miller, C., Moczydlowski, E., Latorre, R. and Phillips, M. (1985) *Nature* 313, 316–318.
- [20] Swartz, K.J. and MacKinnon, R. (1997) *Neuron* 18, 665–673.
- [21] Swartz, K.J. and MacKinnon, R. (1997) *Neuron* 18, 675–682.
- [22] Gurrola, G.B., Rosati, B., Rocchetti, M., Pimienta, G., Zaza, A., Arcangeli, A., Olivotto, M., Possani, L.D. and Wanke, E. (1999) *FASEB J.* 13, 953–962.
- [23] Scaloni, A., Bottiglieri, C., Ferrara, L., Corona, M., Gurrola, G.B., Batista, C., Wanke, E. and Possani, L.D. (2000) *FEBS Lett.* 479, 156–157.
- [24] Hezberg, I.M., Trudeau, M.C. and Robertson, G.A. (1998) *J. Physiol.* 511, 3–14.
- [25] Doyle, D.A., Morais Cabral, J., Pfuetzner, R.A., Kuo, A., Gulbis, J.M., Cohen, S.L., Chait, B.T. and MacKinnon, R. (1998) *Science* 280, 69–77.
- [26] Tseng, G.N. (2001) *J. Mol. Cell Cardiol.* 33, 835–849.